Design of a Sliding Mode Controller for a Macpherson Suspension System to Simulate an LQR-Optimized Skyhook Model

Ali Emran Yazdani[1] and Soroush Abyaneh[2,*]

[1] Department of Mechanical Engineering, Azad University, Chalous, Iran
[2] Department of Mechanical Engineering, Sharif University of Technology, Tehran, Iran
Email: emranyazdani@gmail.com (A.E.Y.); s_abyaneh@alum.sharif.edu (S.A.)
*Corresponding author

***Abstract*—The purpose of this research is to design and implement a controller to achieve a desired displacement and velocity of a sprung mass in a suspension system dynamic model of a vehicle at certain times. In numerous applications, the dynamic response of the Skyhook model is considered the optimal response of a suspension system. As a result, in this project, the response of the Skyhook model is first improved by use of an LQR controller, and then using the sliding mode controller, the response of the realistic car model, represented by a Macpherson suspension system, is adjusted to the response of the LQR-controlled Skyhook model. In order to improve the performance of the suspension, the control force of the actuator in the Macpherson model is obtained by the sliding mode control method, via changing the order of the sliding surface equation. It has been proven that as the system response is optimized in the same way as that of the Skyhook template model with the LQR controller for various road disturbance functions.**

***Keywords*—LQR, macpherson, skyhook control, sliding mode control, suspension system, modelling**

I. Introduction

Among the most essential characteristics of cars is their handling performance. The suspension and tire subsystems in vehicles are considered key elements in the dynamic modeling process while they contribute significantly to the model's dynamic response [1]. The suspension system is a link between the car and its wheels, which basically supports the body weight and provides proper contact between the tire and the ground, as well as the reduction of excitations incurred by the road [2] which will lead to passengers' comfort [3]. Due to this reason, attention to the design and control of suspension systems has become a favorite topic of automobile engineers, as well as increasing the stability of the car motion with the use of semi-active [4, 5] and active suspension systems [6, 7].

To achieve a certain level of comfort, a suspension system should render the car's body movement independent from the bumpiness of the ground. This is generally fulfilled by a passive suspension system consisting of a set of mechanical elements consisting of springs and dampers [8]. However, these elements are unable to adapt to variations in the terrain and hence, a predetermined response would be normally achieved. In compensation for this limitation, active and semi-active suspension systems have been introduced. Active suspension systems, which apply force through an actuator, have proven to be capable to reduce vertical passengers' acceleration and improve the ride quality [9, 10], if implemented in coordination with an effective control strategy [11].

Sam *et al.* [12] used the sliding mode control method for the linear quarter model of a car and finally, they compared the results with an optimal control method. The robustness favorability of sliding mode controllers to uncertainties used in suspension systems have also been reported by Chio *et al.* [13] and Wang *et al.* [14]. Considerable research has been accomplished in the context of active suspension systems robust control with sliding mode [15, 16] and fuzzy controllers [17, 18] as well. Du *et al.* [19] applied the robust control theory as another prevailing control method in the design of active suspension system controllers, with the inclusion of operator's delay in the system modeling. Svaricek *et al.* [20] employed an adaptive robust control for a time-invariant semi-active suspension system. The desired force signal, as a function of the estimated suspended mass, is obtained using the H∞ controller. Finally, the performance of the proposed controller has been compared with the Skyhook algorithm, which shows a satisfactory response. The skyhook control strategy, in which a virtual damper is placed between the sprung mass and the stationary sky, as a means to dampen the undesired vibratory motion of the suspended mass and as a tool to determine the expected damping force, has been introduced by Karnopp *et al.* [21]. A variety of novel

Manuscript received May 28, 2023; revised June 7, 2023; accepted September 27, 2023; published January 26, 2024.

control methods have been developed to implement this strategy [22, 23].

Hurel *et al.* [24] discussed the fundamental development of a two-dimensional non-linear mathematical model of the MacPherson suspension system. This model includes the wheel mass, the moment of inertia about the longitudinal axis of the wheel, the geometry of the suspension and the lateral stiffness of the tire, which allows the analysis of kinematic parameters such as the camber angle. Finally, the results are verified by comparison of the presented model with the model created in the ADAMS software. Balkin *et al.* [25] studied the dynamic and kinematic modeling of the passive dual Wishbone suspension system and compared their results with a general model. Akbari *et al.* [26] applied an observer along with the sliding mode control strategy to a suspension system. Hong *et al.* [27] investigated a MacPherson suspension system with an adaptive control. The control strategy will adjust the gains with regard to the road conditions by use of a conventional skyhook control scheme. Furthermore, the utilization of heuristic methods such as metaheuristic algorithms or neural networks together with sliding mode, adapted for suspension systems leads to promising solutions as well [28, 29]. Hedrick [30] investigated the adaptive semi-active suspension system with the desired Skyhook behavior for a Macpherson dynamic model.

Despite a wide variety of suspension systems modelling in the literature, there has not been a specific focus on the comparison of different models' behaviors and the application of various control strategies to reduce the speed, acceleration and jerk of the sprung and unsprung masses. Therefore in this research, by considering the rotational movement of the unsprung mass in dynamic equations, a conventional, a Skyhook and a Macpherson dynamic model for a suspension system have been developed. In addition, a control algorithm based on the Linear Quadratic Regulator (LQR) has been proposed to improve the system performance of the optimized Skyhook model. Finally, an observer is added for unavailable system's states estimation.

II. System Modelling

Since the requirement of any engineering research is the desire for industrial goals, in this research, a control system based on three suspension system models will be investigated. Therefore, in this section, the response of the conventional suspension system, the MacPherson suspension system, and an optimized Skyhook suspension system are obtained.

A. Conventional Mode

This system consists of a sprung mass and an unsprung mass as in Fig. 1, for which state variables are defined in Eq. (1).

$$\boldsymbol{x} = [x_1 \quad x_2 \quad x_3 \quad x_4]^T = [z_s \quad \dot{z_s} \quad z_u \quad \dot{z_u}]^T \tag{1}$$

The corresponding dynamic equations of this system are as follows:

$$\dot{x_1} = x_2$$
$$\dot{x_2} = -\frac{k_s}{m_s}(x_1 - x_3) - \frac{c_p}{m_s}(x_2 - x_4) \tag{2}$$
$$\dot{x_3} = x_4$$
$$\dot{x_4} = \frac{k_s}{m_u}(x_1 - x_3) + \frac{c_p}{m_u}(x_2 - x_4) + \frac{k_t}{m_u}(z_r - x_3)$$

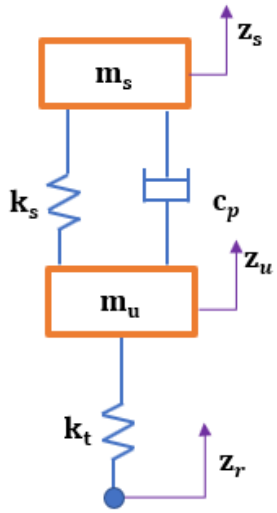

Fig. 1. The conventional suspension system

Hence, the matrix coefficients $\boldsymbol{A_C}$ and $\boldsymbol{B_C}$, of the state space equation governing the conventional suspension system represented as $\dot{\mathbf{x}} = \boldsymbol{A_C}\mathbf{x} + \mathbf{B_C}z_r$, are:

$$A_C = \begin{bmatrix} 0 & 1 & 0 & 0 \\ -\frac{k_s}{m_s} & -\frac{c_p}{m_s} & \frac{k_s}{m_s} & \frac{c_p}{m_s} \\ 0 & 0 & 0 & 1 \\ \frac{k_s}{m_u} & \frac{c_p}{m_u} & \frac{-(k_s+k_t)}{m_u} & \frac{-c_p}{m_u} \end{bmatrix} \tag{3}$$

$$B_C = \begin{bmatrix} 0 & 0 & \frac{k_t}{m_u} & 0 \end{bmatrix}^T \tag{4}$$

B. Macpherson Model

The quarter car model of a Macpherson suspension system, introduced in [27] is shown schematically in Fig. 2.

First, the coordinates of points B and C are specified as key points:

$$y_B = l_B(\cos(\theta - \theta_0) - \cos(-\theta_0)) \tag{5}$$
$$z_B = z_s + l_B(\sin(\theta - \theta_0) - \sin(-\theta_0)) \tag{6}$$
$$y_C = l_C(\cos(\theta - \theta_0) - \cos(-\theta_0)) \tag{7}$$
$$z_C = z_s + l_C(\sin(\theta - \theta_0) - \sin(-\theta_0)) \tag{8}$$

where $l_B = \overline{OB}$, $l_C = \overline{OC}$ and $l_A = \overline{OA}$. The initial angular position of the unsprung mass is denoted by θ_0. $\tilde{\alpha}$ is the summation of θ_0 and α. The distance between points A and B could be calculated, which is the main difference between the dynamic equations of the conventional and MacPherson suspension systems and would result in a more realistic model.

$$l = \sqrt{{l_A}^2 + {l_B}^2 - 2l_A l_B cos\ \tilde{\alpha}} \tag{9}$$

$$\tilde{I} = \sqrt{{l_A}^2 + {l_B}^2 - 2l_A l_B \cos(\tilde{\alpha} - \theta)} \tag{10}$$

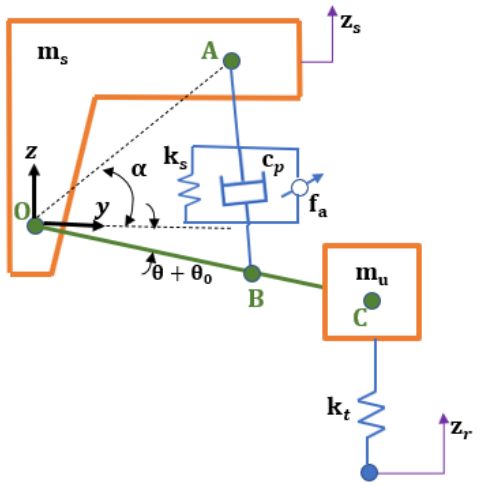

Fig. 2. The quarter car model of a Macpherson suspension system.

In these equations, l indicates the initial distance between A and B, and $\tilde{I}$ is the displacement between A and B from the equilibrium point (taking into account the counterclockwise rotation of the unsprung mass which is the chassis). Therefore, the spring deflection (Δl), the displacement rate of the piston inside the damper ($\dot{\Delta l}$), and the change of the shape of the tire have been obtained by the following relations respectively.

$$\begin{aligned}\Delta l^2 = (l - \tilde{I})^2 = 2a_l - b_l(cos\tilde{\alpha} + \cos(\tilde{\alpha} - \theta)) \\ - 2\{{a_l}^2 - a_l b_l(cos\tilde{\alpha} \\ + \cos(\tilde{\alpha} - \theta) \\ + {b_l}^2 cos\tilde{\alpha}\cos(\tilde{\alpha} - \theta)\}^{\frac{1}{2}}\end{aligned} \tag{11}$$

$$\dot{\Delta l} = \dot{I} - \dot{\tilde{I}} = \frac{b_l \sin(\tilde{\alpha} - \theta)\dot{\theta}}{2\sqrt{(a_l - b_l \cos(\tilde{\alpha} - \theta))}} \tag{12}$$

$$z_C - z_r = z_s + l_C(\sin(\theta - \theta_0) - \sin(-\theta_0)) - z_r \tag{13}$$

where $a_l = \sqrt{{l_A}^2 + {l_B}^2}$ and $b_l = 2l_A l_B$.

To investigate the dynamic characteristics of the suspension system, Lagrange equations will be used, hence the kinetic energy (T), the potential energy (V) and the dissipation energy (D) are first determined as follows:

$$T = \frac{1}{2}m_s \dot{z_s}^2 + \frac{1}{2}m_u(\dot{y_C}^2 - \dot{z_C}^2) \tag{14}$$

$$V = \frac{1}{2}k_s \Delta l^2 + \frac{1}{2}k_t(z_C - z_r)^2 \tag{15}$$

$$D = \frac{1}{2}c_P \dot{\Delta l}^2 \tag{16}$$

After substitution of Eqs. (11)–(13) into Eqs. (14)–(16), the following equations are derived:

$$T = \frac{1}{2}(m_s + m_u)\dot{z_s}^2 + \frac{1}{2}m_u {l_C}^2 \dot{\theta}^2 + m_u l_C \cos(\theta)\dot{\theta}\,\dot{z_s} \tag{17}$$

$$\begin{aligned}V = \frac{1}{2}k_s[2a_l - b_l(\cos\tilde{\alpha} + \cos(\tilde{\alpha} - \theta)) \\ - 2\{{a_l}^2 - a_l b_l(\cos\tilde{\alpha} \\ + \cos(\tilde{\alpha} - \theta) \\ + {b_l}^2 \cos\tilde{\alpha}\cos(\tilde{\alpha} - \theta)\}^{\frac{1}{2}}]^2 \\ + \frac{1}{2}k_t(z_s \\ + l_C(\sin(\theta - \theta_0) \\ - \sin(-\theta_0)) - z_r)^2\end{aligned} \tag{18}$$

$$D = \frac{c_P[b_l \sin(\tilde{\alpha} - \theta)\,\dot{\theta}]^2}{8(a_l - b_l \cos(\tilde{\alpha} - \theta))} \tag{19}$$

Lagrange Eq. (20) for obtaining differential equations of the Macpherson suspension system model with generalized coordinates defined as $q_1 = z_s$ and $q_2 = \theta$.

$$\frac{d}{dt}\left(\frac{\partial T}{\partial \dot{q}_i}\right) + \frac{\partial D}{\partial \dot{q}_i} + \frac{\partial V}{\partial q_i} = Q_i, \qquad i = 1,2 \tag{20}$$

Substituting Eqs. (17)–(19) in Eq. (20), the governing differential equations are calculated as:

$$\begin{aligned}(m_s + m_u)\ddot{z_s} + m_u l_C cos(\theta - \theta_0)\ddot{\theta} \\ - m_u l_C sin(\theta - \theta_0)\dot{\theta}^2 \\ + k_t(z_s \\ + l_C(\sin(\theta - \theta_0) \\ - \sin(-\theta_0)) - z_r) = 0\end{aligned} \tag{21}$$

$$\begin{aligned}{m_u l_C}^2 \ddot{\theta} + m_u l_C \cos(\theta - \theta_0)\ddot{z_s} \\ + \frac{c_P {b_l}^2 \sin(\tilde{\alpha} - \theta)\,\dot{\theta}}{4(a_l - b_l \cos(\tilde{\alpha} - \theta))} \\ + k_t l_C \cos(\theta - \theta_0)(z_s \\ + l_C(\sin(\theta - \theta_0) \\ - \sin(-\theta_0)) - z_r) \\ - \frac{1}{2}k_s l_C \sin(\tilde{\alpha} - \theta)\left[b_l \right. \\ \left. + \frac{d_l}{\sqrt{c_l - d_l \cos(\tilde{\alpha} - \theta)}}\right] \\ = -l_B f_a\end{aligned} \tag{22}$$

where $c_l = {a_l}^2 - a_l b_l \cos(\alpha + \theta_0)$ and $d_l = a_l b_l - {b_l}^2 \cos(\alpha + \theta_0)$. By considering the following state variables:

$$[x_1, x_2, x_3, x_4]^T = [z_s, \dot{z_s}, \theta, \dot{\theta}]^T \tag{23}$$

The state-space representation of these differential equations could be written as:

$$\begin{aligned}\dot{x_1} = x_2 \\ \dot{x_2} = f_1(x_1, x_2, x_3, x_4, f_a, f_d, z_r) \\ \dot{x_3} = x_4 \\ \dot{x_4} = f_2(x_1, x_2, x_3, x_4, f_a, f_d, z_r)\end{aligned} \tag{24}$$

where f_1 and f_2 have been defined in [27].

Linearization

By linearizing the nonlinear system around the equilibrium point using the Taylor expansion, the linear, time-variant and continuous state space equations of the Macpherson suspension system are expressed as follows:

$$\dot{x}(t) = A_{Mc}x(t) + B_{Mc1}f_a(t) + B_{Mc2}z_r(t), \quad x(0) = x_0 \tag{25}$$

$$y(t) = Cx(t)$$

where

$$\mathbf{A_{Mc}} = \begin{bmatrix} 0 & 1 & 0 & 0 \\ \frac{\partial f_1}{\partial x_1} & \frac{\partial f_1}{\partial x_2} & \frac{\partial f_1}{\partial x_3} & \frac{\partial f_1}{\partial x_4} \\ 0 & 0 & 0 & 1 \\ \frac{\partial f_2}{\partial x_1} & \frac{\partial f_2}{\partial x_2} & \frac{\partial f_2}{\partial x_3} & \frac{\partial f_2}{\partial x_4} \end{bmatrix} \tag{26}$$

$$\mathbf{B_{Mc1}} = \begin{bmatrix} 0 & \frac{\partial f_1}{\partial f_a} & 0 & \frac{\partial f_2}{\partial f_a} \end{bmatrix}^T_{f_a=0} \tag{27}$$

$$= \begin{bmatrix} 0 \\ \frac{l_B \cos(-\theta_0)}{m_s l_C + m_u l_C \sin^2(-\theta_0)} \\ 0 \\ \frac{l_B(m_s + m_u)}{m_s m_u {l_C}^2 + {m_u}^2 {l_C}^2 \sin^2(-\theta_0)} \end{bmatrix}$$

$$\mathbf{B_{Mc2}} = \begin{bmatrix} 0 & \frac{\partial f_1}{\partial z_r} & 0 & \frac{\partial f_2}{\partial z_r} \end{bmatrix}^T_{z_r=0} \tag{28}$$

$$= \begin{bmatrix} 0 \\ \frac{k_t l_C \sin^2(-\theta_0)}{m_s l_C + m_u l_C \sin^2(-\theta_0)} \\ 0 \\ \frac{l_C m_s k_t \cos(-\theta_0)}{(m_s m_u {l_C}^2 + {m_u}^2 {l_C}^2 \sin^2(-\theta_0)} \end{bmatrix}$$

C. Skyhook Model with an LQR Controller

In this section, assuming the use of the quarter car model, a modified Skyhook suspension system model with an LQR controller is studied as demonstrated in Fig. 3.

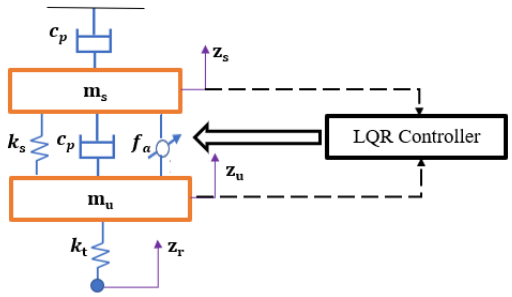

Fig. 3. The modified Skyhook suspension system model with an LQR controller.

The progressiveness of this model as an ideal reference model is explained as follows:

Firstly, the state variables of the Skyhook suspension system are considered in the form of the following equation:

$$[x_1, x_2, x_3, x_4]^T = [z_s, \dot{z}_s, z_u, \dot{z}_u]^T \tag{29}$$

Secondly, the state-space representation of the corresponding differential equations is derived as per Eq. (30):

$$\dot{x_1} = x_2$$

$$\dot{x_2} = -\frac{k_s}{m_s}(x_1 - x_2) - \frac{c_p}{m_s}(x_2 - x_4) \pm \frac{c_p}{m_s}x_2 + \frac{f_a}{m_s} \tag{30}$$

$$\dot{x_3} = x_4$$

$$\dot{x_4} = \frac{k_s}{m_u}(x_1 - x_2) + \frac{c_p}{m_u}(x_2 - x_4) + \frac{k_t}{m_u}(z_r - x_3) - \frac{f_a}{m_u}$$

The matrices $\boldsymbol{A_{S-h}}$, $\boldsymbol{B_{1S-h}}$ and $\boldsymbol{B_{2S-h}}$ for the state space equation governing the Skyhook suspension system represented as $\dot{\mathbf{x}} = \boldsymbol{A_{S-h}}\mathbf{x} + \boldsymbol{B_{1S-h}}, z_r + \boldsymbol{B_{2S-h}}, f_a$, are:

$$\mathbf{A_{S-h}} = \begin{bmatrix} 0 & 1 & 0 & 0 \\ -\frac{k_s}{m_s} & -\frac{2c_p}{m_s} & \frac{k_s}{m_s} & \frac{c_p}{m_s} \\ 0 & 0 & 0 & 1 \\ \frac{k_s}{m_u} & \frac{c_p}{m_u} & \frac{-(k_s+k_t)}{m_u} & \frac{-c_p}{m_u} \end{bmatrix} \tag{31}$$

$$\mathbf{B_{1S-h}} = \begin{bmatrix} 0 & 0 & \frac{k_t}{m_u} & 0 \end{bmatrix}^T \tag{32}$$

$$\mathbf{B_{2S-h}} = \begin{bmatrix} 0 & \frac{1}{m_s} & 0 & \frac{1}{m_u} \end{bmatrix}^T \tag{33}$$

The response of this model to the disturbance from the road is usually considered to be the optimal response. The justification for the adopted structure in Fig. 3 is as follows: The control algorithm must stabilize the depicted 2DoF system by using an actuator. The actuator performance is restricted and its dynamics is quite challenging. Moreover, with fixed gains, the two control objectives, which are improvement of both the vehicle driving performance and ride quality, cannot be met. Therefore, to better improve the response of this system, an optimal control strategy based on an LQR for the introduced mathematical model is proposed.

LQR controller

The optimal control input $u(t)$, is a state variable feedback regulator expressed as [31]:

$$\mathbf{u} = -\mathbf{K}\mathbf{x} \tag{34}$$

The optimization process involves the calculation of the optimal control input that will minimize the performance index J, which is defined as follows:

$$\mathbf{J} = \int_0^\infty (\mathbf{x^T Q x} + \mathbf{u^T R u})\, dt \tag{35}$$

The first term in the above equation denotes the requirement for the performance characteristics and the second term is due to the optimal control input limitations. For the minimization of the performance index, the matrix gain should be defined as the following [32]:

$$\mathbf{K} = \mathbf{R^{-1}B^{T}P} \tag{36}$$

where $\boldsymbol{P}$ is the solution to the following reduced-matrix Riccati equation:

$$\mathbf{A^{T}P + PA - PBR^{-1}B^{T}P + Q = 0} \tag{37}$$

In order to get the desired response from the sprung mass, the term related to the position of the sprung mass in the Q matrix has been chosen equal to 100,000. As a result, considering the Q and R weight matrices as the following:

$$\mathbf{Q} = \begin{bmatrix} 100000 & 0 & 0 & 0 \\ 0 & 1 & 0 & 0 \\ 0 & 0 & 1000 & 0 \\ 0 & 0 & 0 & 1 \end{bmatrix}, \mathbf{R = I} \tag{38}$$

The optimal state variables feedback controller for the Skyhook system will be defined as:

$$\mathbf{U} = -\left(\mathbf{R^{-1}B^{T}P}\right)\mathbf{x} \tag{39}$$

III. Numerical Example

In order to simplify the relations, it is assumed that $l_B = l_A\cos(\alpha)$, $l_C = l_B$ and $\theta_0 = 0$. As a result, the state space matrix coefficients defined by the Eqs. (26)–(28) are obtained as:

$$\mathbf{A_{Mc}} = \begin{bmatrix} 0 & 1 & 0 & 0 \\ 0 & 0 & \frac{k_s l_C}{m_s} & \frac{c_p l_C}{m_s} \\ 0 & 0 & 0 & 1 \\ \frac{-k_t}{m_u l_C} & 0 & \frac{-(m_s+m_u)k_s}{m_s m_u} - \frac{k_t}{m_u} & \frac{-(m_s+m_u)c_p}{m_s m_u} \end{bmatrix} \tag{40}$$

$$B_{Mc1} = \begin{bmatrix} 0 & \frac{1}{m_s} & 0 & \frac{-(m_s+m_u)}{m_s m_u l_C} \end{bmatrix}^T \tag{41}$$

$$B_{Mc2} = \begin{bmatrix} 0 & 0 & 0 & \frac{k_t}{m_u l_C} \end{bmatrix}^T \tag{42}$$

The following values are considered for the parameters described by the corresponding state space equations for the three models as shown in Table I.

TABLE I. The Simplified Macpherson Model Parameters

Parameter	Value (unit)
m_s	453 kg
k_s	17658 N/m
c_p	1950 Ns/m
m_u	71 kg
k_t	18388 M/m
l_C	0.37 m

A step function, denoted by z_r in Fig. 4, as the road disturbance has been applied to all three models in order to compare the systems' behavior. The position of the sprung and unsprung masses could be seen in Figs. 4 and 5 respectively.

As can be observed from these figures, although the unsprung mass vibrates almost the same in all three models, the sprung mass oscillations for the Skyhook model with the LQR controller demonstrates a favorable response with a less overshoot and a faster settling time for a road disturbance with a step function. As a matter of fact, by comparison of the Macpherson model and the Skyhook model with the LQR controller, the latter model's overshoot has been reduced by 68% and its settling time has been enhanced from 3 s to 2 s (34% enhancement).

Another road disturbance input with a bump-shaped function is used for the suspension system models and the positions of the sprung and unsprung masses are demonstrated in Figs. 6 and 7 respectively.

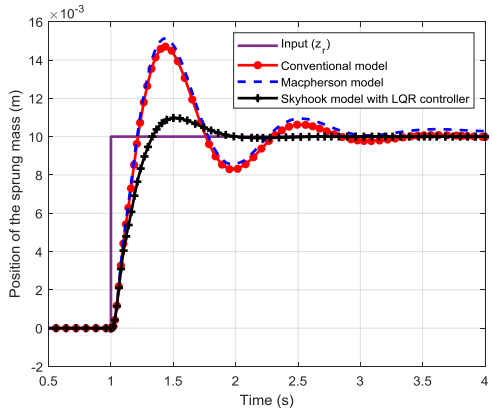

Fig. 4. Position of the sprung mass (z_s) in the conventional, Macpherson and Skyhook suspension system models with a step road disturbance.

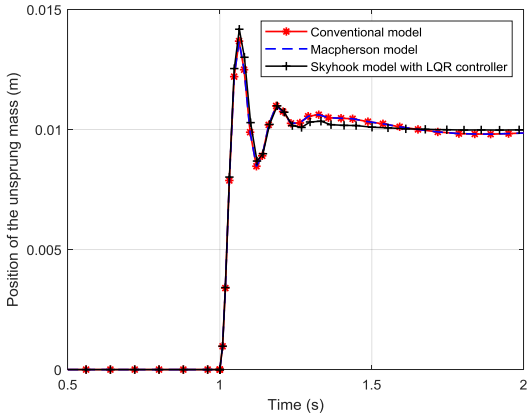

Fig. 5. Position of the unsprung mass (z_u) in the conventional, Macpherson and Skyhook suspension system models with a step road disturbance.

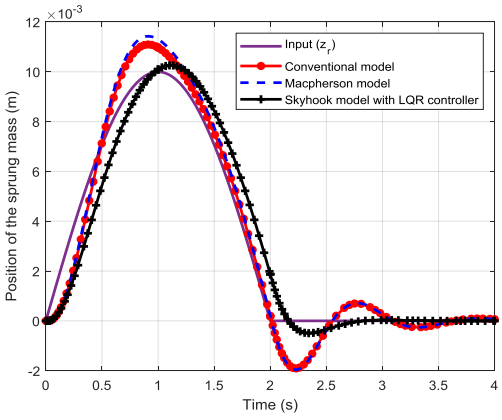

Fig. 6. Position of the sprung mass (z_s) in the conventional, Macpherson and Skyhook suspension system models with a bump road disturbance.

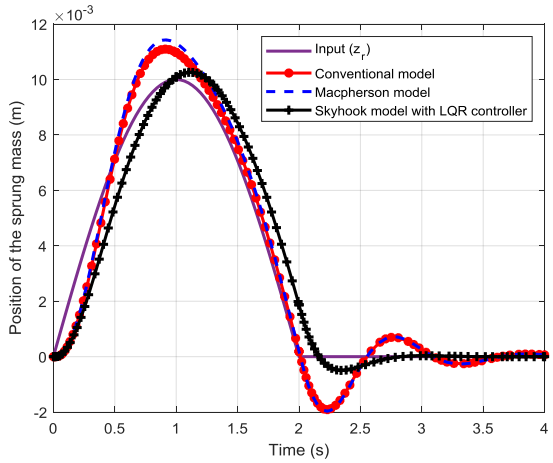

Fig. 7. Position of the unsprung mass (z_u) in the conventional, Macpherson and Skyhook suspension system models with a bump road disturbance.

The deviation of the sprung and unsprung mass response from the road input for all these 3 models are shown in Table II.

TABLE II. THE SIMPLIFIED MACPHERSON MODEL PARAMETERS

Model	Deviation for the unsprung mass (%)	Deviation for the sprung mass (%)
Conventional	23	22
Macpherson	22	21
Skyhook	13	12

The second case also confirms the fact that unsprung mass oscillations are the same for the suspension system models but the sprung mass vibrations vary for these models. The sprung mass response in the Skyhook model with the LQR controller shows the best behavior as it smoothly converges to the road input function with the least error compared to the other models.

IV. CONTROL INPUT DESIGN WITH A SLIDING MODE CONTROLLER

In this section, a control input for the Macpherson suspension system model is to be designed so that the model behavior follows that of a desired model. In the previous section, it was proven that the Skyhook suspension system model, optimized by an LQR controller, exhibited the preferred response which will be referred to as the desired system in this section. So, the control input design with the sliding mode control method, to achieve the desired dynamic behavior of the LQR-optimized skyhook model will be discussed.

A common sliding surface expression is as follows, which depends on only one scalar parameter, λ.

$$\mathbf{S} = (\frac{\mathrm{d}}{dt} + \lambda)^n \tilde{\mathrm{x}} \tag{43}$$

where the error $\tilde{\mathrm{x}}$, as defined bellow, is the difference between the sprung mass displacement of the Macpherson model (x_{Mc}) and that of the ideal model (x_{S-h}), which is the Skyhook system with the LQR controller.

$$\tilde{x} = \mathrm{x}_{Mc} - \mathrm{x}_{S-h} \tag{44}$$

If the sliding surface differential equation order is chosen to be $n = 2$, the sliding surface in Eq. (43) can be rewritten as:

$$\begin{aligned} S = (\frac{\mathrm{d}}{dt} + \lambda)^2 \tilde{x} \Rightarrow S &= (D + \lambda)^2 \tilde{x} \\ &= (D^2 + 2\lambda D + \lambda^2)\tilde{x} \\ &= (\ddot{\mathrm{x}}_{Mc} - \ddot{\mathrm{x}}_{S-h}) + 2\lambda\dot{\tilde{x}} + \lambda^2 \tilde{x} \end{aligned} \tag{45}$$

From the linearized Macpherson dynamic equations, $\ddot{\mathrm{x}}_M$ will be the following equation:

$$\ddot{\mathrm{x}}_{Mc} = 14.42\theta + 1.592\dot{\theta} + 0.0022 f_a(t) \tag{46}$$

By substituting Eq. (46) into Eq. (45), the control signal is derived as follows:

$$f_a(t) = \frac{1}{0.0022}(\ddot{\mathrm{x}}_{S-h} - 14.42\theta - 1.592\dot{\theta} - 2\lambda\dot{\tilde{x}} - \lambda^2\tilde{x}) \tag{47}$$

The comparison of the Macpherson suspension system response with the obtained control input and the LQR-controlled Skyhook suspension system, as the ideal model, are shown in the following figures to the step road disturbance shown in Fig. 8. Figs. 8 and 9 illustrate the sprung mass displacement and velocity of both models respectively.

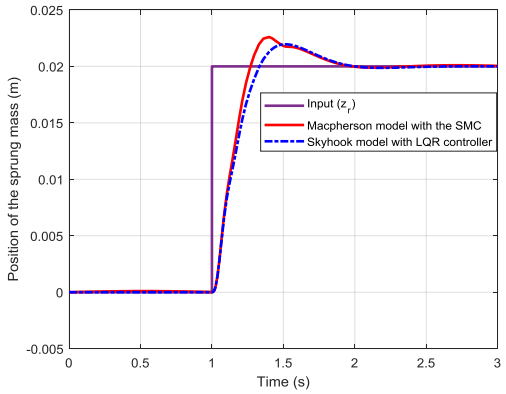

Fig. 8. Sprung mass positions (z_u) of the Macpherson model with the sliding mode controller and the Skyhook model with the LQR controller to a step road disturbance (z_r).

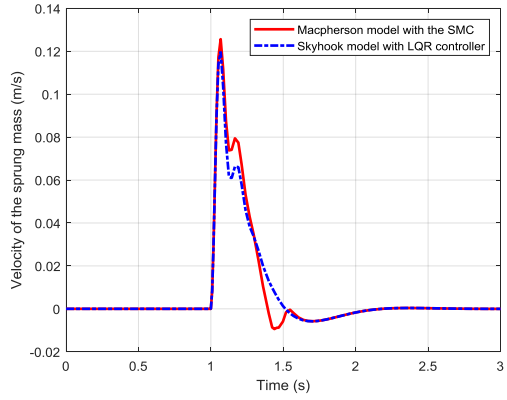

Fig. 9. Sprung mass velocites ($\dot{z}_u$) of the Macpherson model with the sliding mode controller and the Skyhook model with the LQR controller to a step road disturbance (z_r).

As is evident from these figures, when the sliding mode controller is applied to the Macpherson suspension system,

the displacement of the sprung mass caused by the road step disturbance, converges acceptably to that of the ideal model (the Skyhook suspension system with an LQR controller). Therefore, the optimization effect of the Macpherson model with the sliding mode controller has been clearly illustrated.

Next, the system response to the road disturbance as defined in Fig. 10 has been obtained as can be seen from Figs. 11 and 12.

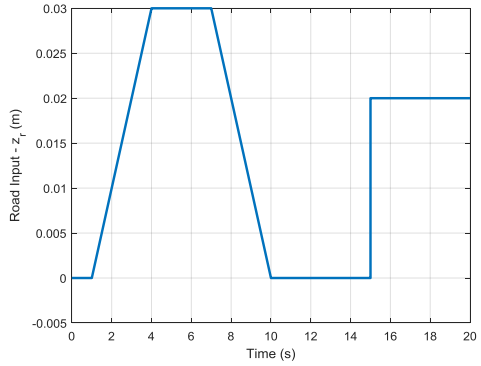

Fig. 10. The second road disturbance (z_r) function.

It is seen that the response convergence of the Macpherson model with the sliding mode controller, both for sprung mass displacement and velocity, to the Skyhook model with the LQR controller has been substantially improved compared to the same results without the SMC.

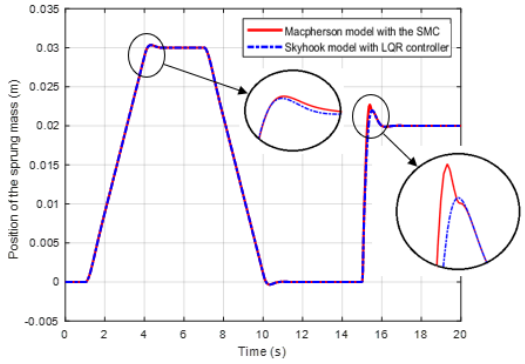

Fig. 11. Sprung mass positions (z_u) of the Macpherson model with the sliding mode controller and the Skyhook model with the LQR controller to the second road disturbance (z_r).

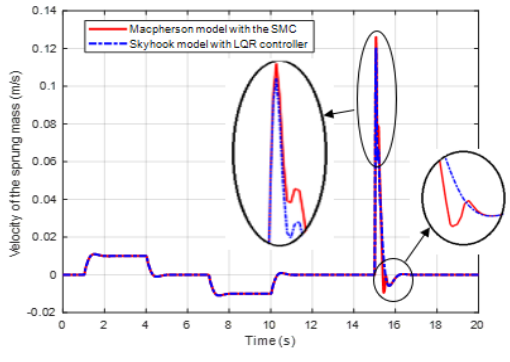

Fig. 12. Sprung mass velocities ($\dot{z}_u$) of the Macpherson model with the sliding mode controller and the Skyhook model with the LQR controller to the second road disturbance (z_r).

V. Conclusion

In this paper, a vehicle suspension system was modeled using three different approaches for the plant's dynamics description namely; the conventional model, the Macpherson model and the Skyhook model with an LQR controller, for which the estimation of the control variables was based on the developed linearized model. After giving two road disturbance functions to as the input to these models, the sprung mass vibrations were compared and the Skyhook model was proved to be sufficiently effective and its performance was competent enough. Hence the Skyook model was chosen as the ideal model for the next step.

In order to improve the Macpherson suspension system model, the control input for the damping force was redesigned using a sliding mode controller. In other words, by using a generalized control input from the sliding mode control method, on the MacPherson suspension system and matching its response with that of the LQR-optimized skyhook model, the verification for the application of this method on the MacPherson suspension system was established. It was determined that the semi-active Macpherson system could achieve a similar control performance as that of the chosen ideal model. The described control strategy can be extended to a verity of semi-active suspension systems.

Conflict of Interest

The authors declare no conflict of interest.

Author Contributions

All authors have contributed to the paper equally. They both conducted the research; analyzed the data; and wrote the paper. All authors had approved the final version.

References

[1] F. He, J. Zhao, and H. Wang, "Study on control strategies of semi-active air suspension for heavy vehicles based on road-friendliness," *Adv. Mater. Res.*, vol. 452, pp. 328–333, 10.4028/scientific5/AMR.452–453.328, 2012.

[2] S. Nguyen, D. Bao, and V. Ngo, "Fractional-order sliding-mode controller for semi-active vehicle MRD suspensions," *Nonlinear Dyn*., vol. 101, pp. 795–821, 2020, https://doi.org/10.1007/s11071-020-05818-w.

[3] Kavitha, S. Shankar, K. Karthika, B. Ashok, and S. Ashok, "Active camber and toe control strategy for the double wishbone suspension system," *J. King Saud Univ.-Eng. Sci.*, vol. 31, no. 4, pp. 375–384, 2019, https://doi.org/10.1016/j.jksues.2018.01.003.

[4] Z. Zhang, J. Wang, W. Wu, and C. Huang, "Semi-active control of air suspension with auxiliary chamber subject to parameter uncertainties and time-delay," *Int. J. Robust. Nonlinear Control*, vol. 30, pp. 7130–7149, https://doi.org/10.1002/rnc.5169, 2020.

[5] R. Wang, W. Liu, R. Ding, X. Meng, Z. Sun, L. Yang, and D. Sun, "Switching control of semi-active suspension based on road profile estimation," *Veh. Syst. Dyn*., pp. 1–21, 2021, https://doi.org/10.1080/00423114.2021.1889621.

[6] S. Savaresi, C. Poussot-Vassal, C. Spelta, O. Sename, and L. Dugard, *Semi-active Suspension Control Design for Vehicles*, Elsevier Ltd., 2011.

[7] Y. Huang, J. Na, X. Wu, G. Gao, and Y. Guo, "Robust adaptive control for vehicle active suspension systems with uncertain dynamics," *Trans. Inst. Meas. Control*, vol. 40, pp. 1237–1249, https://doi.org/10.1177/0142331216678312, 2018.

[8] L. Ovalle, H. R ós, and H. Ahmed, "Robust control for an active suspension system via continuous sliding-mode controllers," *Eng. Sci. and Tech., an International Journal*, vol. 28, p. lhttps://doi.org/10.1016/j.jestch.2021.06.006, 2022.
[9] M. Yatak and F. Sahin, "Ride comfort-road holding trade-off improvement of full vehicle active suspension system by interval type-2 fuzzy control," *Eng. Sci. Technol. Int. J.*, vol. 24, no. 1, pp. 259–270, https://doi.org/10.1016/j.jestch.2020.10.006, 2021.
[10] K. Rajeswari and P. Lakshmi, "PSO optimized fuzzy logic controller for active suspension system," in *Proc. International Conference on Advances in Recent Technologies in Communication and Computing, IEEE*, 2010, pp. 278–283, 10.1109/ARTCom.2010.22.
[11] T. Yang, N. Sun, Y. Fang, X. Xin, and H. Chen, "New adaptive control methods for n-link robot manipulators with online gravity compensation: design and experiments," *IEEE Trans. Industr. Electron*, vol. 1, https://doi.org/10.1109/TIE.2021.3050371, 2021.
[12] Y. Sam, J. Osman, and M. Ghani, "A class of proportional-integral sliding model control with application to active suspension system," *J. Sys. and Control*, vol. 51, no. 3, pp. 217–223, https://doi.org/10.1016/j.sysconle.2003.08.007, 2004.
[13] S. Choi, J. Choi, Y. Lee, and M. Han, "Vibration control of an ER seat suspension for a commercial vehicle," *J. Dyn. Syst. Meas. Control*, vol. 125, pp. 60–68, https://doi.org/10.1115/1.1542639, 2003.
[14] G. Wang, M. Chadli, and M. Basin, "Practical terminal sliding mode control of nonlinear uncertain active suspension systems with adaptive disturbance observer," *IEEE/ASME Trans. Mechatron*, vol. 26, pp. 789–797, https://doi.org/10.1109/TMECH.2020.3000122, 2020.
[15] R. Kothandaraman, L. Satyanarayana, and L. Ponnusamy, "Grey fuzzy sliding mode controller for vehicle suspension system," *J. Control Eng. Appl. Inf.*, vol. 17, no. 3, pp. 12–19, 2015.
[16] H. Ahmed and H. R ós, "Experimental study of robust output-based continuous sliding-modes controllers for Van der Pol oscillator," *IET Control Theory Appl.*, vol. 12, no. 15, pp. 2088–2097, 2018.
[17] Qazi, C. de Silva, A. Khan, and M. Khan, "Performance analysis of a semiactive suspension system with particle swarm optimization and fuzzy logic control," *Scientific World J.*, https://doi.org/10.1155/2014/174102, 2014.
[18] T. Yang, N. Sun, and Y. Fang, "Adaptive fuzzy control for a class of MIMO underactuated systems with plant uncertainties and actuator deadzones," *Design and Experiments, IEEE Trans. Cybern*., pp. 1–14, 2021, https://doi.org/10.1109/TCYB.2021.3050475.
[19] H. Du and N. Zhang, "H∞ control of active vehicle suspension with actuator time delay," *J. Sound and Vibration*, vol. 301, no. 1, pp. 236–252, https://doi.org/10.1016/j.jsv.2006.09.022, 2007.
[20] Svaricek and M. Ahmed, "Adaptive robust gain scheduled control of vehicle semi-active suspension for improved ride comfort and road handling," *ICMECH*, pp. 376–381, 2013.
[21] D. C. Karnopp, M. J. Crosby, and R. A. Harwood, "Vibration control using semi-active force generators," *ASME J. Eng. Ind.*, vol. 96, no. 2, pp. 619–626, 1974, https://doi.org/10.1115/1.3438373.
[22] M. Valasek, M. Novak, and O. Vaculin, "A new concept of semi-active control of trucks suspension," in *Proc. of AVEC 96, International Symposium on Advanced Vehicle Control, Aachen University of Technology*, pp. 141–151, 1996, https://doi.org/10.1080/00423119708969333.
[23] H. Besinger, D. Cebon, and D. J. Cole, "Force control of a semi-active damper," *Veh. Syst. Dyn*., vol. 24, pp. 695–723, 1995, https://doi.org/10.1080/00423119508969115.
[24] J. Hurel, A. Mandow, and A. Garcia-Cerezo, "Nonlinear two-dimensional modeling of a McPherson suspension for kinematics and dynamics simulation," in *Proc. 12th IEEE International Workshop on Advanced Motion Control (AMC)*, 2012, pp. 1–6, https://doi.org/10.1109/AMC.2012.6197009.
[25] K. Balike, S. Rakheja, and I. Stiharu, "Development of kineto-dynamic quarter-car model for synthesis of a double wishbone suspension," *International Journal of Vehicle Mechanics and Mobility*, vol. 49, pp. 107–128, 2011, https://doi.org/10.1080/00423110903401905.
[26] E. Akbari, M. Farsadi, I. Z. Mat Darus, and R. Ghelichi, "Observer design for active suspension system using sliding mode control," in *Proc. IEEE Student Conference on Research and Development (SCOReD)*, Kuala Lumpur, Malaysia, 2010, 10.1109/SCORED.2010.5704003.
[27] K. Hong, H. Sohn, and J. K. Hedrick, "Modified skyhook control of semi-active suspensions: A new model, gain scheduling, and hardware-in-the-loop tuning," *ASME. J. Dyn. Sys., Meas., Control*, vol. 124, no. 1, pp. 158–167, 2002, https://doi.org/10.1115/1.1434265.
[28] J. Fei, H. Wang, and Y. Fang, "Novel neural network fractional-order sliding-mode control with application to active power filter," *IEEE Trans. Syst. Man Cybern.: Syst*., pp. 1–11, 2021, https://doi.org/10.1109/TSMC.2021.3071360.
[29] J. Fei, Y. Chen, L. Liu, and Y. Fang, "Fuzzy multiple hidden layer recurrent neural control of nonlinear system using terminal sliding-mode controller," *IEEE Trans. Cybern.*, pp. 1–16, 2021, https://doi.org/10.1109/TCYB.2021.3052234.
[30] J. Hedrick, "Modified skyhook control of semi-active suspensions: A new model, gain scheduling, and Hardware-in-the-Loop tuning," *Transactions of the ASME*, vol. 124, pp. 158–167, 2002, https://doi.org/10.1115/1.1434265.
[31] L. Gopala Rao and S. Narayanan, "Sky-hook control of nonlinear quarter car model traversing rough road matching performance of LQR control," *Journal of Sound and Vibration*, vol. 323, pp. 515–529, https://doi.org/10.1016/j.jsv.2009.01.025, 2009.
[32] Y. M. Sam, M. R. H. A. Ghani, and N. Ahmad, "LQR controller for active car suspension," in *Proc. TENCON Intelligent Systems and Technologies for the New Millennium* (Cat. No.00CH37119), Kuala Lumpur, Malaysia, vol. 1, 2000, pp. 441–444, doi: 10.1109/TENCON.2000.893707.